ADVANCED FUNCTIONAL MATERIALS

FULL PAPER

DOI: 10.1002/adfm.200600759

# Reversible Hydrogen Storage by a Li–Al–N–H Complex

By *Zhitao Xiong*, *Guotao Wu*, *Jianjiang Hu*, *Yongfeng Liu*, *Ping Chen*,* *Weifang Luo*, and *James Wang*

Stepwise solid-state reaction between $LiNH_2$ and $LiAlH_4$ at a molar ratio of 2:1 is investigated in this paper. It is observed that approximately four H atoms are evolved from a mixture of $LiNH_2$–$LiAlH_4$ (2:1) after mechanical ball milling. The transformation of tetrahedral $[AlH_4]^-$ in $LiAlH_4$ to the octahedral $[AlH_6]^{3-}$ in $Li_3AlH_6$ is observed after ball milling $LiAlH_4$ with $LiNH_2$. Al–N bonding is identified by using solid-state $^{27}Al$ nuclear magnetic resonance (NMR) measurements. The NMR data, together with the results of X-ray diffraction and Fourier transform IR measurements, indicate that a Li–Al–N–H intermediate with the chemical composition of $Li_3AlN_2H_4$ forms after ball milling. Heating the post-milled sample to 500 °C results in the liberation of an additional four H atoms and the formation of $Li_3AlN_2$. More than 5 wt % hydrogen can be reversibly stored by $Li_3AlN_2$. The hydrogenated sample contains $LiNH_2$, LiH, and AlN. The role of AlN in the reversible hydrogen storage over Li–Al–N–H is discussed.

## 1. Introduction

Rapid development in fuel-cell technologies focuses attention on the development of suitable hydrogen-storage materials with high storage capacity and fast kinetics for on-board applications.[1] It has been demonstrated that the safest and most effective way of hydrogen storage is by using solid media.[2] A few promising solid-state systems, such as complex hydrides,[3–5] metal organic frameworks,[6,7] and so forth, have been proposed and are under intensive investigation. A metal–N–H system, a new candidate for hydrogen storage, has attracted considerable attention over the past few years. From the binary Li–N–H system[8] to the ternary Li–Mg–N–H, Li–Ca–N–H, and Mg–Na–N–H systems,[9–14] significant progress has been made towards practical applications. As an example, the temperature for hydrogen desorption from Li–Mg–N–H is considerably lowered compared to that of Li–N–H; the desorption plateau pressure increases from 1 bar (1 bar = 100 000 Pa) at ca. 275 °C for Li–N–H to ca. 20 bar at 180 °C for Li–Mg–N–H.[9,12]

Previous investigations on metal–N–H systems revealed that mixtures of amide and binary hydrides of alkali and alkaline earth metals were capable of releasing hydrogen under certain conditions. It is likely that the Coulombic attraction between $H^{\delta+}$ in amides and $H^{\delta-}$ in hydrides induces hydrogen desorption from the mixtures.[9,15] Based on this interpretation, such interactions would be expected between amides and complex hydrides, such as $NaAlH_4$, $LiAlH_4$, and $LiBH_4$. $LiAlH_4$ has long been the subject of research as a potential hydrogen-storage medium because of its high hydrogen content.[16,17] It consists of a $Li^+$ cation and an $AlH_4^-$ anion. The hydrogen atoms in the $AlH_4^-$ anion are tetrahedrally coordinated to the Al atom and have a distinct electron-rich character.[18] Attempts for hydrogen release have been made using $LiNH_2$–$LiAlH_4$ and $NaNH_2$–$LiAlH_4$ systems.[19,20] Fast hydrogen release was observed from the mixture of $LiAlH_4$ and $NaNH_2$ upon ball milling, that is, four H atoms per [1 $NaNH_2$–1 $LiAlH_4$] were detached from the mixture within ten minutes.[21] Unfortunately, the reaction was exothermic which is irreversible for the reverse process of hydrogenation under practical conditions. The reaction between $LiNH_2$ and $LiAlH_4$ (amide/hydride molar ratio = 1:1) is a mildly endothermic process liberating approximately four H atoms per [1 $LiNH_2$–1 $LiAlH_4$] after ten hours of ball milling. However, the recharging of the dehydrogenated samples was unsuccessful at hydrogen pressures of up to 80 bar.[22] Relevant work was also reported by Nakamori et al. without giving details about hydrogen release during ball milling and structural identification.[23] More recently, Jun and Fang investigated a mixture of $LiNH_2$ and $LiAlH_4$ in a molar ratio of 1:2, and reported that $LiNH_2$ effectively destabilized $LiAlH_4$ by reacting with LiH during the dehydrogenation process of $LiAlH_4$.[24] $LiBH_4$ can also react with $LiNH_2$. More than 10 wt % of hydrogen can be released upon heating a mixture of $LiNH_2$ with $LiBH_4$ at a molar ratio of 2:1.[25] Apparently, introducing complex hydrides into the amide–hydride systems could bring interesting results for the development of a metal–N–H system as a hydrogen-storage medium.

In this paper the interaction between $LiNH_2$ and $LiAlH_4$ at a molar ratio of 2:1 was investigated. Hydrogen release during

[*] Dr. P. Chen, Dr. Z. Xiong, Dr. G. Wu, Dr. J. Hu, Dr. Y. Liu
Department of Physics, Faculty of Science
National University of Singapore
10 Kent Ridge Crescent, Singapore 117542 (Singapore)
E-mail: phychenp@nus.edu.sg
Dr. P. Chen
Department of Chemistry, Faculty of Science
National University of Singapore
10 Kent Ridge Crescent, Singapore 117543 (Singapore)
Dr. W. Luo, Dr. J. Wang
Sandia National Laboratories
Analytical Material Science Department, MS 9403
7011 East Ave, Livermore, CA 94550 (USA)

ball milling and subsequent heating processes were carefully monitored and measured by using a pressure gauge and volumetric gas reaction controller. In addition, phase and structural changes were analyzed by using X-ray diffraction (XRD), Fourier transform IR (FTIR), and solid-state $^{27}Al$ nuclear magnetic resonance (NMR). Rehydrogenation of the dehydrogenated sample was also conducted.

## 2. Results and Discussion

### 2.1. Dehydrogenation of the $LiNH_2$–$LiAlH_4$ (Molar Ratio 2:1) Sample

A gaseous product was generated in a vessel shortly after ball milling a mixture of $LiNH_2$–$LiAlH_4$ (2:1). The pressure within the ball-mill vessel was measured by using a pressure gauge at different ball-milling intervals. Mass spectrometry analyses conducted at all checkpoints revealed that hydrogen was the only detectable gaseous product. The $NH_3$ concentration was below 80 ppm, as determined by using a Metrohm 781 pH/Ion Meter at the end of the ball milling. According to the ideal equation of state, the approximate amount of hydrogen evolved from the mixture can be calculated. The results are shown in Figure 1. It can be seen that 1.05 H, 1.96 H, and 2.98 H atoms were evolved from the mixture after 40, 65, and 180 min of ball milling, respectively. In total 4.02 H atoms

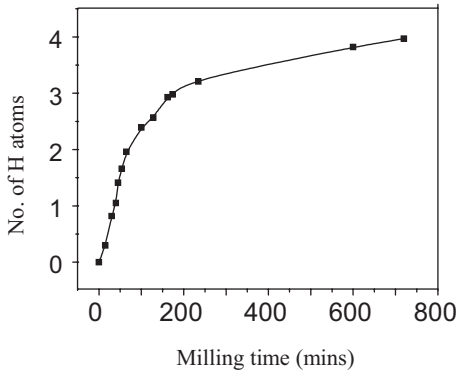


**Figure 1.** Number of equivalent hydrogen atoms evolved from a mixture of $LiNH_2$–$LiAlH_4$ (2:1) during the milling process.

were evolved from the starting compounds after 12 h of ball milling (the purities of the starting chemicals have been taken into consideration). $LiAlH_4$ and $LiNH_2$ were also milled individually under the same conditions for the purpose of comparison. $LiNH_2$ was stable against ball milling, that is, little gaseous product was detected by using mass spectrometry and no phase change was identified by using XRD. As for $LiAlH_4$, no pressure increase inside the vessel was detectable after 12 h of ball milling, which agrees well with the literature report that mechanically induced solid-state transformation of $LiAlH_4$ is difficult.[26]

Figure 2 shows the XRD patterns of $LiNH_2$–$LiAlH_4$ (2:1) samples collected at different intervals of milling. The $Li_3AlH_6$

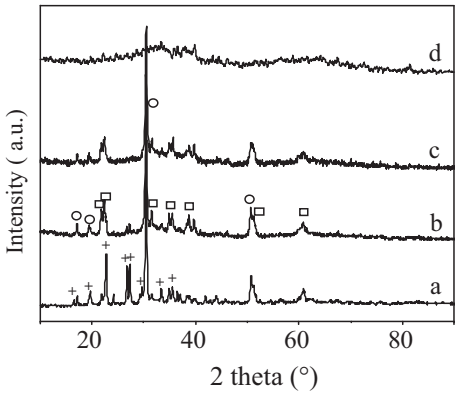


**Figure 2.** XRD patterns of the post-milled $LiNH_2$–$LiAlH_4$ (2:1) samples with a) 1.05, b) 1.96, c) 2.98, and d) 4.02 H atoms detached per [2 $LiNH_2$–1 $LiAlH_4$]. Peaks marked with + are the characteristic diffraction peaks of $LiAlH_4$, □—$Li_3AlH_6$, ○—$LiNH_2$.

phase can be identified clearly after milling the mixture for 40 min revealing the transformation of tetrahedral $[AlH_4]^-$ to octahedral $[AlH_6]^{3-}$ (Fig. 2a). The diffraction peaks of $LiAlH_4$ gradually weakened and finally disappeared as ball milling progressed (Fig. 2b and c). The $Li_3AlH_6$ phase, on the other hand, gradually developed initially, and then, disappeared later. At the end of the milling treatment no clear phase could be identified except for two broad bands in the ranges of 20° to 40° and 50° to 70°, indicating the existence of amorphous phase(s) (Fig. 2d). No metallic Al phase was detected during the milling process.

According to literature,[27,28] $LiAlH_4$ converts to $Li_3AlH_6$, Al, and $H_2$ at temperatures above 140 °C. $Li_3AlH_6$ further decomposes to Al, LiH, and $H_2$ at temperatures above 190 °C. The highly endothermic reaction between Al and LiH gives LiAl and $H_2$ at temperatures above 400 °C. The stepwise thermal decomposition of $LiAlH_4$ is described by Equation 1.

$$LiAlH_4 \rightarrow 2/3\,Al + 1/3\,Li_3AlH_6 + H_2 \rightarrow Al + LiH + 3/2\,H_2 \rightarrow LiAl + 2\,H_2 \quad (1)$$

Although with the same number of H atoms (approximately four H atoms) detached from the reactant(s), the chemical process between $LiNH_2$ and $LiAlH_4$, which occurs during ball milling, exhibits distinct differences from the thermal decomposition of pure $LiAlH_4$, that is, hydrogen desorption occurred at much reduced temperatures and no metallic Al or LiAl phase was formed. It is inferred that $LiNH_2$ participates, which changes the reaction path and thermodynamics for hydrogen desorption.

To investigate the behavior of $LiNH_2$ in hydrogen desorption and identify the unknown amorphous product formed after milling, FTIR was employed to monitor the variation of N–H stretch in the post-milled samples. It can be seen in Figure 3 that the N–H stretches in $LiNH_2$ at 3313 and 3258 $cm^{-1}$ were gradually weakened with ball milling. New vibrations at 3295 and 3240 $cm^{-1}$ gradually developed (Fig. 3d), which cannot be assigned to any known Li–N–H compounds and may originate from the newly formed amorphous phase. The doublet feature

ADVANCED FUNCTIONAL MATERIALS



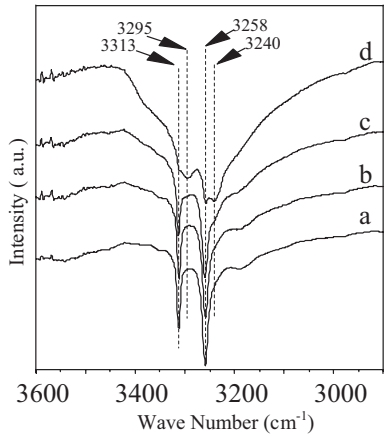


**Figure 3.** FTIR spectra of a post-milled $LiNH_2$–$LiAlH_4$ (2:1) sample with a) 1.05, b) 1.96, c) 2.98, and d) 4.02 atoms detached per mixture.

of the new absorbance indicates that the $-NH_2$ group may be incorporated in the post-milled mixture.

As the solid residue is of an amorphous nature, little information can be derived from XRD measurements. Solid-state magic-angle spinning NMR (MAS NMR) was then employed to investigate the chemical environments of Al, Li, and H. Figure 4I shows the $^{27}Al$ NMR spectra of the solid residues of $LiNH_2$–$LiAlH_4$ (2:1) collected at different intervals of ball milling. $^{27}Al$ NMR spectra of $LiAlH_4$ and AlN were also recorded as references. It can be seen that the evolution of a $LiNH_2$–$LiAlH_4$ (2:1) sample with 1.05 H atoms displayed two dominant $^{27}Al$ NMR peaks at –35 and 95 ppm, respectively. The symmetrical peak centered at –35 ppm can be assigned to Al in six-coordinated $AlH_6$ sites[29] which reveals the formation of $Li_3AlH_6$, agreeing with the XRD results. Prolonging ball-milling treatment, $[AlH_6]^{3-}$ was first enhanced and then finally

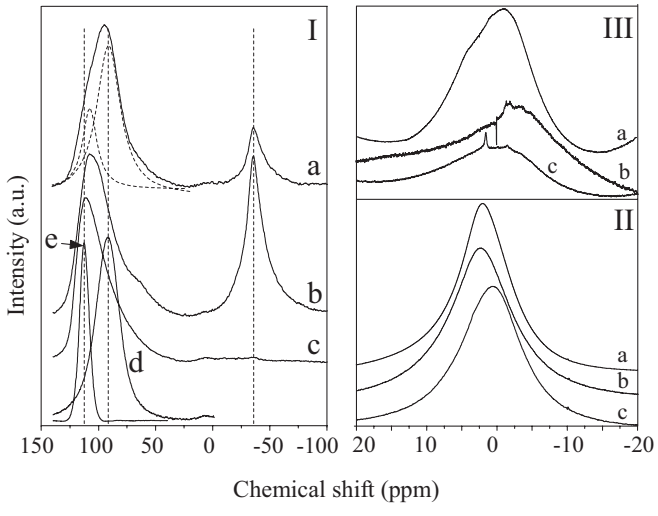


**Figure 4.** $^{27}Al$ MAS NMR spectra of I) a post-milled $LiNH_2$–$LiAlH_4$ (2:1) sample with a) 1.05, b) 2.98, and c) 4.02 H atoms evolved per mixture, d) $LiAlH_4$, and e) AlN. II,III) $^7Li$ and $^1H$ MAS NMR spectra of a) a post-milled $LiNH_2$–$LiAlH_4$ (2:1) sample with 4.02 H atoms evolved, b) $LiNH_2$, and c) LiH.

disappeared. The asymmetric peak at 95 ppm can be resolved into two peaks at 108 and 93 ppm. The peak at 93 ppm corresponds to Al in four-coordinated $AlH_4$ sites of $LiAlH_4$.[29] While the peak at 108 ppm is new and is in a chemical shift region between four H-coordinated Al (93 ppm) in $LiAlH_4$ and four N-coordinated Al (112 ppm) in AlN. It is concluded that the Al at 108 ppm may have a four-coordinated ($AlH_{4-x}N_x$) environment. A similar deduction was made by Fitzgerald et al. when investigating the chemical reaction between AlN and $Al_2O_3$.[30] In their study a new $^{27}Al$ resonance at 106 ppm, a chemical shift between that of local $AlO_4$ (65 ppm) and $AlN_4$ (112 ppm), was assigned empirically to the four-coordinated aluminum oxynitride ($AlO_{4-x}N_x$). With an increase of the milling time, the broad asymmetric peak at 95 ppm moved higher to 110 ppm, which is close to the chemical shift of AlN. The resonance at 93 ppm gradually weakened due to consumption of $LiAlH_4$. At the end of the milling the majority of Al was in the $AlN_4$ coordination environment. The asymmetry of the peak may be due to the part of Al remaining in ($AlH_{4-x}N_x$). No metallic Al with a chemical shift around 1640 ppm[29] was observed in all of the post-milled samples, which is consistent with the XRD results. $^7Li$ NMR spectra (Fig. 4II) of the post-12 h-milled sample has a broad symmetric peak centered at 2.01 ppm, which differs from that of $LiNH_2$ (at 2.38 ppm) and LiH (at 0.54 ppm). Hydrogen in the solid residue has two chemical environments, that is, one is hydridelike (at ca. 3.97 ppm) and the other is amidelike (at ca. 0.97 ppm) (Fig. 4IIIa). It is concluded that part of the H may coordinate with Li and Al and other H atoms bond with N in the form of $-NH_2$.

It can be concluded from the solid NMR analyses that the Al–N bonds were formed following the ball milling, which may result from the interaction between $LiNH_2$ and $LiAlH_4$. It is likely that the N in $LiNH_2$ (as electron donor) donates a lone pair to the empty orbit of Al in $LiAlH_4$ (as electron acceptor) to establish Coulombic donor–acceptor attraction. As two species in close contact such attraction may weaken the Al–H bonding and expel H from Al. As a consequence, $LiAlH_4$ converts to $Li_3AlH_6$. $LiNH_2$ may continuously react with $Li_3AlH_6$ so that most of the Al bonds with N rather than H. Most of the H atoms previously bonded with Al were evolved as $H_2$. At the same time considerable chemical changes of Li and H in $LiNH_2$ occurred. From the number of H atoms evolved from the starting reactants and the XRD and FTIR results, the chemical process occurring during the ball-milling treatment can be described by Equation 2.

$$2\,LiNH_2 + LiAlH_4 \rightarrow [Li_3AlN_2H_4] + 2\,H_2 \qquad 4.76\ wt\,\% \qquad (2)$$

From the chemical composition point of view, $Li_3AlN_2H_4$ is likely to be a mixture of $LiNH_2 + AlN + 2LiH$. However, the solid product is difficult to identify by using XRD due to its poor crystallinity. The formula of $[Li_3AlN_2H_4]$ will be kept in Equation (2). More detailed investigations are given below.

Because there are four more H atoms in the solid residue, that is, $[Li_3AlN_2H_4]$, considerable hydrogen desorption is expected at higher temperatures. Quantitative measurement of

  

the hydrogen desorption was conducted using a volumetric analyzer by heating the post-milled sample to 500 °C. As shown in Figure 5a hydrogen desorption begins at a temperature immediately above 50 °C. Mass spectrometry analysis revealed that hydrogen is the only gaseous product. At the end of the

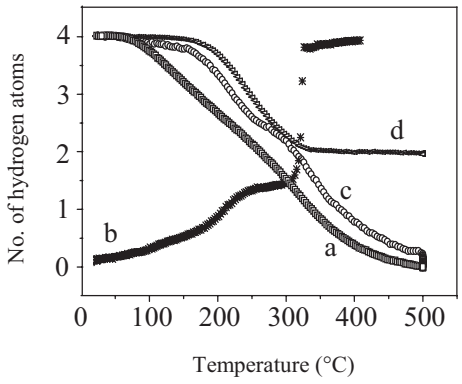


**Figure 5.** Volumetric measurements of a) hydrogen release from post-12h-milled $LiNH_2$–$LiAlH_4$ (2:1) sample, b) hydrogen absorption over $Li_3AlN_2$, c) hydrogen desorption from the fully hydrogenated $Li_3AlN_2$ sample, and d) hydrogen release from the $LiNH_2$–LiH (1:2) mixture.

heating nearly four H atoms were desorbed from the $[Li_3AlN_2H_4]$. Together with the amount of hydrogen released during the ball-milling process, ca. 8H atoms were evolved from the $LiAlH_4$-$LiNH_2$ (2:1) mixture. As expected, the final solid product was $Li_3AlN_2$, which was identified by using XRD (Fig. 6a). The overall reaction of hydrogen release from a $LiNH_2$–$LiAlH_4$ (2:1) mixture can, thus, be described by using Equation 3.

$$2\,LiNH_2 + 1\,LiAlH_4 \rightarrow [Li_3AlN_2H_4] + 2\,H_2 \rightarrow Li_3AlN_2 + 4\,H_2 \quad 9.5\ wt\,\% \qquad (3)$$

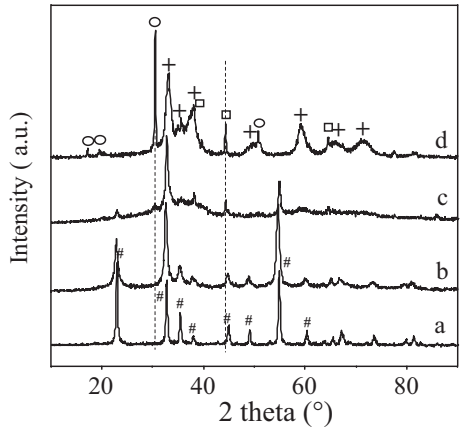


**Figure 6.** XRD patterns of a) a fully dehydrogenated $LiNH_2$–$LiAlH_4$ (2:1) sample (release to 500 °C), b) rehydrogenation to 200 °C, c) 280 °C, and d) 330 °C (hydrogen pressure 80 bar). Peaks marked with # are the characteristic diffraction of $Li_3AlN_2$, □—LiH, +—AlN, ○—$LiNH_2$

### 2.2. Hydrogenation of $Li_3AlN_2$

Hydrogenation of $Li_3AlN_2$ was performed under a hydrogen pressure of 80 bar. As shown in Figure 5b the absorption process took place in two steps, that is, initial uptake began at around 60 °C and slowly reached 1.97 wt % at 250 °C. Little hydrogen was absorbed in the temperature range of 250–270 °C. Only after the temperature increased to 280 °C can absorption be accelerated and an additional 3.2 % of weight gain was gained. Altogether 5.17 wt % of hydrogen or about four H atoms per $Li_3AlN_2$ molecule were absorbed by $Li_3AlN_2$. It should be noted that in a previous investigation by Yamane et al. the hydrogenation of $Li_3AlN_2$ at temperatures up to 300 °C under 100 bar of $H_2$ was not observed.[31]

To understand the phase transitions which occur during the hydrogenation of $Li_3AlN_2$, partially hydrogenated (at 200 °C and 280 °C), fully hydrogenated $Li_3AlN_2$ samples were collected for XRD and NMR measurements. As shown in Figure 6b, no significant change in the XRD pattern was observed after $Li_3AlN_2$ was hydrogenated at 200 °C despite the slight broadening of the diffraction peaks. While solid-state $^{27}Al$ NMR gave a new resonance at 122 ppm, which was in coexistence with the dominant peak at 114 ppm, that is, Al in $Li_3AlN_2$ (Fig. 7b). The 122 ppm signal corresponds to a new type of Al with a distinct chemical environment. It should be noted that $LiAl(NH_2)_4$ possesses a similar chemical shift (121 ppm, Fig. 7e), indicating that Al within the partially hydrogenated sample is likely to be coordinated with $–NH_2$ groups. After hydrogenation at 280 °C, the $Li_3AlN_2$ phase greatly decreased as shown by XRD patterns. $LiNH_2$ and LiH appeared and developed (Fig. 6c). In accordance with the XRD result, NMR disclosed that the dominant Al resonance shifted to 112 ppm, that is, Al in AlN. The resolved shoulder peak at around 122 ppm was enhanced to some extent; however, such an Al-containing product is undetectable by using

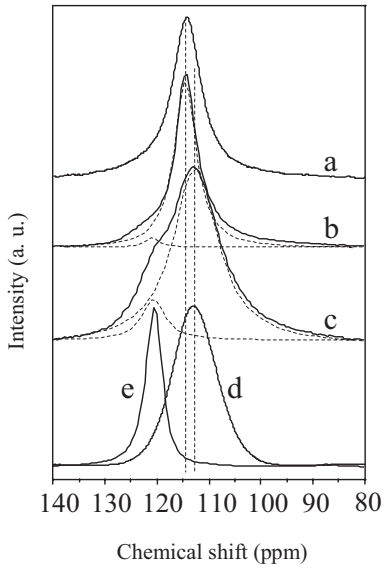


**Figure 7.** $^{27}Al$ MAS NMR spectra of a) $Li_3AlN_2$ and its hydrogenated samples collected at b) 200 °C, c) 280 °C, d) 330 °C (fully hydrogenation state), and e) ternary amide $LiAl(NH_2)_4$.

ADVANCED FUNCTIONAL MATERIALS



XRD, indicating an amorphous nature. At the end of hydrogenation an AlN phase was detected by using XRD but with rather broad peaks indicating poor crystallinity. The assumption of Al completely in an $AlN_4$ environment of AlN (112 ppm) was also supported by a solid-state $^{27}$Al NMR measurement. Therefore, the fully hydrogenated sample contains $LiNH_2$, LiH, and AlN. The hydrogenation of $Li_3AlN_2$ can be described by Equation 4.

$$Li_3AlN_2 + 2\,H_2 \rightarrow LiNH_2 + 2\,LiH + AlN \quad \Delta H = -50.1\ kJ\,mol^{-1}\,H_2 \tag{4}$$

It should be noted that the chemical composition of the hydrogenated sample is identical to the post-milled sample, that is, $[Li_3AlNH_4]$; it is likely that the $[Li_3AlNH_4]$ is in a metastable state formed under high-energy ball milling in which the chemical environments of Li, Al, N, and H exhibit certain differences from those in an unmilled mixture of $LiNH_2$, LiH, and AlN.

Hydrogen desorption from the fully hydrogenated $Li_3AlN_2$ occurred at temperatures above 100 °C. As shown in Figure 5c, the liberation of hydrogen increased monotonically with temperature. After heating to 500 °C, four H atoms evolved. XRD measurements confirmed that the dehydrogenation product had the $Li_3AlN_2$ structure showing the full reversibility of the reaction in Equation 4.

### 2.3. Thermodynamic Analyses

Thermodynamic analyses were performed on the reactions in Equations 3 and 4. The standard enthalpies of formation of $LiAlH_4$, $LiNH_2$, $Li_3AlN_2$, AlN, and LiH are –113, –176, –568, –311, and –91 kJ mol$^{-1}$,[32–34] respectively. Therefore, the enthalpy change of the reaction in Equation 3 is –25.8 kJ mol$^{-1}$-$H_2$. The exothermic nature of the reaction reveals that upon hydrogenation $Li_3AlN_2$ cannot return to $LiNH_2$ and $LiAlH_4$ under practical conditions. For the reaction in Equation 4 the enthalpy is –50.1 kJ mol$^{-1}$-$H_2$, which further confirms the reversible nature observed by the volumetric and XRD measurements.

It is interesting to compare the reaction in Equation 4 with the hydrogenation of $Li_3N$, that is, the reaction in Equation 5.

$$Li_3N + 2\,H_2 \rightarrow LiNH_2 + 2\,LiH \qquad \Delta H = -80.5\ kJ\,mol^{-1}\text{-}H_2 \tag{5}$$

The difference lies in the involvement of AlN, which either associates with $Li_3N$ in the form of the ternary nitride or remains as one of the products. Volumetric release of $H_2$ was also determined on the hydrogenated $Li_3N$ sample, that is, $LiNH_2 + 2LiH$. As shown in Figure 5d, dehydrogenation of $LiNH_2 + 2LiH$ was observed in the temperature range of 150–500 °C, two H atoms were evolved under the experimental conditions, which is consistent with the theoretical value of the dehydrogenation to an imide phase, that is, $LiNH_2 + 2\,LiH \rightarrow Li_2NH + LiH + H_2$. In the volumetric measurement hydrogen desorbed was accumulated gradually inside the testing chamber, as a result, hydrogen pressure of ca. 0.3 bar presented in the system at the end of measurement. The second step of desorption in Li–N–H, that is, $Li_2NH + LiH \rightarrow Li_3N + H_2$, can not proceed under this condition. However, under the same conditions a mixture of $LiNH_2 + 2\,LiH + AlN$ releases all four H atoms and returns to the nitride phase. Clearly, the more stable nature of $Li_3AlN_2$ compared with $Li_3N + AlN$ (i.e., $Li_3N + AlN \rightarrow Li_3AlN_2$ $\Delta H = -30.4$ kJ mol$^{-1}$) is responsible for the considerable change in the thermodynamics. Similar changes were found recently by Vajo et al.[35] in the reduction of the dehydrogenation temperatures of LiH and $MgH_2$ by introducing Si. The alteration of chemical compositions of hydrogen-storage materials is, therefore, an effective method to optimize the thermodynamics of the absorption and desorption processes.

## 3. Conclusions

Continuous chemical environment changes of Al, namely from $[AlH_4]$, $[AlH_6]$, and $[AlN_xH_{4-x}]$ to [AlN], in the dehydrogenation of $LiNH_2$–$LiAlH_4$ (2:1) were detected by using solid-state $^{27}$Al NMR. Equivilents of approximately four H atoms were released after ball milling a mixture of $LiNH_2$–$LiAlH_4$ (2:1) for 12 h. Heating the post-milled sample to high temperatures resulted in the desorption of an additional four H atoms and formation of $Li_3AlN_2$. A new coordination state of Al was formed during the hydrogenation of $Li_3AlN_2$. $LiNH_2$, LiH, and AlN were identified to be the fully hydrogenated products. Therefore, 5.17 wt % of hydrogen can be reversibly stored by $Li_3AlN_2$ in the temperature range of 50–500 °C. Considerable thermodynamic improvements on the reaction of $LiNH_2 + 2LiH$ were achieved with the presence of AlN.

## 4. Experimental

Fine powders of $LiNH_2$ and $LiAlH_4$ were purchased from Sigma–Aldrich and Fluka with claimed purites of 95 and 97 %, respectively. A $LiNH_2$–$LiAlH_4$ mixture with a molar ratio of 2:1 was loaded to the custom-made mill vessel inside a glovebox and ball milled using a Retsch PM400 planetary mill at 200 rpm. The ball-to-sample weight ratio was about 30:1. To reduce the heat effect by milling, the mill was set to revolve for 60 s in one direction and pause 30 s, and then revolve in reversal direction. Thanks to the ventilation device inside the compartment of the mill no obvious temperature increase was directly detected. After milling for a given time the custom-made mill vessel equipped with gas valves was connected to a pressure gauge to measure the internal pressure. As $H_2$, $N_2$, and $NH_3$ are the likely gaseous products, the gas evolved during ball milling was firstly analyzed by using a mass spectrometer and then, slowly introduced to 30 mL distilled water to collect $NH_3$. A Metrohm 781 pH/Ion Meter (Switzerland) equipped with an $NH_3$-selective electrode was employed to determine the concentration of ammonium ions ($NH_4^+$) in the aqueous solution. The lower limit of detection is 0.1 ppm. To prevent air contaminations all sample handling was performed within a MBRAUN glovebox filled with purified argon.

Quantitative measurements of hydrogen desorption and subsequent absorption by post-milled samples were performed on a commercial gas reaction controller provided by Advanced Materials Corporation. An approximately 500 mg sample was employed for each experiment and the heating rate was 1 K min$^{-1}$.

Solid-state NMR measurements were carried out at 9.7 Tesla on a Bruker Advance 400 NMR spectrometer operating at 104.2 MHz for $^{27}$Al, at 155.4 MHz for $^{7}$Li, and at 400 MHz for $^{1}$H. Samples were

  

packed in 4 mm MAS zirconia rotors with a Kel-F cap inside the glovebox. NMR spectra were acquired in a Cross-Polarization (CP)/MAS probe using single-pulse excitation and a rotor-spinning rate of 10 kHz. Chemical shifts ($\delta$) were referenced to a 1 M aqueous solution of aluminum nitrate, lithium chloride, and TMS.

Structural identifications were performed by using a Bruker X-ray diffractometer equipped with an in situ cell. XRD data were collected from 10° to 90° in $2\theta$ with a scan-step width of 0.01° using Cu K$\alpha$ radiation. FTIR spectra were recorded by a Perkin–Elmer 3000 FTIR spectrometer at room temperature. Diffuse reflectance IR Fourier Transform (DRIFT) mode was applied.

Received: August 18, 2006
Revised: November 23, 2006
Published online: March 8, 2007

[1] F. Schuth, B. Bogdanovic, M. Felderhoff, *Chem. Commun.* **2004**, 2249.
[2] L. Schlapbach, A. Zuttel, *Nature* **2001**, *414*, 353.
[3] B. Bogdanovic, M. Schwickardi, *J. Alloys Compd.* **1997**, *253*, 1.
[4] C. Jensen, K. Gross, *Appl. Phys. A: Mater. Sci. Process.* **2001**, *72*, 213.
[5] G. Sandrock, K. Gross, G. Thomas, *J. Alloys Compd.* **2002**, *339*, 299.
[6] S. S. Kaye, J. R. Long, *J. Am. Chem. Soc.* **2005**, *127*, 6506.
[7] N. L. Rosi, J. Eckert, M. Eddaoudi, D. T. Vodak, J. Kim, M. O'Keeffe, O. M. Yaghi, *Science* **2003**, *300*, 1127.
[8] P. Chen, Z. T. Xiong, J. Z. Luo, J. Y. Lin, K. L. Tan, *Nature* **2002**, *420*, 302.
[9] Z. T. Xiong, G. T. Wu, J. J. Hu, P. Chen, *Adv. Mater.* **2004**, *16*, 1522.
[10] Z. T. Xiong, J. J. Hu, G. T. Wu, P. Chen, *J. Alloys Compd.* **2005**, *395*, 209.
[11] Z. T. Xiong, J. J. Hu, G. T. Wu, P. Chen, W. F. Luo, K. Gross, J. Wang, *J. Alloys Compd.* **2005**, *398*, 235.
[12] W. F. Luo, *J. Alloys Compd.* **2004**, *381*, 284.
[13] H. Y. Leng, T. Ichikawa, S. Hino, N. Hanada, S. Isobe, H. Fujii, *J. Phys. Chem. B* **2004**, *108*, 8763.
[14] Y. Nakamori, S. Orimo, *J. Alloys Compd.* **2004**, *370*, 271.
[15] P. Chen, J. Luo, Z. Xiong, J. Lin, K. L. Tan, *J. Phys. Chem. B* **2003**, *107*, 10 967.
[16] E. Finholt, A. C. Bond, H. I. Schlesinger, *J. Am. Chem. Soc.* **1947**, *69*, 1199.
[17] N. Sklar, B. Post, *Inorg. Chem.* **1967**, *6*, 669.
[18] J. W. Lauher, D. Dougherty, P. Herley, *Acta Crystallogr.* **1979**, *B35*, 1454.
[19] P. Chen, presented at *A Variety of Metal–N–H Systems for Hydrogen Storage, Session P14: Focus Session: Hydrogen Storage I: Media*, Los Angeles, CA, March **2005**.
[20] Z. T. Xiong, G. T. Wu, J. J. Hu, P. Chen, presented at *Symp. P Materials for Rechargeable Batteries, Hydrogen Storage and Fuel Cells; 3rd Int. Conf. on Materials for Advanced Technologies (ICMAT 2005) and 9th Int. Conf. on Advanced Materials (ICAM 2005)*, Singapore, July **2005**.
[21] Z. T. Xiong, G. T. Wu, J. J. Hu, P. Chen, *Catal. Today* **2007**, *120*, 287.
[22] Z. T. Xiong, G. T. Wu, J. J. Hu, P. Chen, *J. Power Sources* **2006**, *159*, 167.
[23] Y. Nakamori, A. Ninomiya, G. Kitahara, M. Aoki, T. Noritake, K. Miwa, Y. Kojima, S. Orimo, *J. Power Sources* **2006**, *155*, 447.
[24] L. Jun, Z. Z. Fang, *J. Phys. Chem. B* **2005**, *109*, 20 830.
[25] F. E. Pinkerton, G. P. Meisner, M. S. Meyer, M. P. Balogh, M. D. Kundrat, *J. Phys. Chem. B* **2004**, *109*, 6.
[26] L. Zaluski, A. Zaluska, J. O. Strom-Olsen, *J. Alloys Compd.* **1999**, *290*, 71.
[27] J. A. Dilts, E. C. Ashby, *Inorg. Chem.* **1972**, *11*, 1230.
[28] J. Block, A. P. Gray, *Inorg. Chem.* **1965**, *4*, 104.
[29] J. W. Wiench, V. P. Balema, V. K. Pecharsky, M. Pruski, *J. Solid State Chem.* **2004**, *177*, 648.
[30] J. J. Fitzgerald, S. D. Kohl, G. Piedra, *Chem. Mater.* **1994**, *6*, 1915.
[31] H. Yamane, T. Kano, A. Kamegawa, M. Shibata, T. Yamada, M. Okada, M. Shimada, *J. Alloys Compd.* **2005**, *402*, L1.
[32] O. M. Lovvik, S. M. Opalka, H. W. Brinks, B. C. Hauback, *Phys. Rev. B: Condens. Matter Mater. Phys.* **2004**, *69*, 134 117.
[33] *Gmelins Handbuch der Anorganischen Chemie, Lithium*, System Number 20 (Ed: R. J. Meyer), Verlag Chemie, Weinhein, Germany **1960**, p. 270–273.
[34] J. M. Mchale, A. Navrotsky, F. J. DiSalvo, *Chem. Mater.* **1999**, *11*, 1148.
[35] J. J. Vajo, F. Mertens, C. C. Ahn, R. C. Bowman, Jr., B. Fultz, *J. Phys. Chem. B* **2004**, *108*, 13 977.